18TH WORLD CONFERENCE ON EARTHQUAKE ENGINEERING
WCEE2024
MILAN

MILAN, ITALY
30TH JUNE - 5TH JULY 2024

www.wcee2024.it

SEISMIC BEHAVIOUR OF MODERN AGGREGATE MASONRY STRUCTURES: A NONLINEAR DYNAMIC ANALYSIS

S. Torres-Olivares[1], B. González-Rodrigo[2], E. I. Saavedra Flores [2], N. Tarque [2], L. Navas-Sánchez [2] & D. Hidalgo-Leiva [3]

[1] Faculty of Engineering, Civil Engineering Department, University of Santiago of Chile, Santiago, Chile

[2] Universidad Politécnica de Madrid, Madrid, Spain

[3] Civil Engineering School, University of Costa Rica, San José, Costa Rica

Abstract: *In this study, we investigate the seismic behaviour of contemporary aggregate masonry structures in high seismic risk areas, with a focus on San José, Costa Rica. Our research highlights the interconnected response of dwellings within structural aggregates and compares them to isolated configurations in seismic events. We employ finite element modelling with multi-layered shell elements to accurately capture the behaviour of reinforced partially grouted concrete block masonry. The model includes vertical and horizontal reinforcements and simulates concrete blocks, grout, and mortar as homogenized layers using the OpenSees software. We validate the model by comparing it with experimental data. Nonlinear multi-directional dynamic analyses are performed to investigate the seismic behaviour of aggregate masonry systems. The proposed model is first evaluated for isolated partially grouted reinforced concrete block masonry, and identical systems are then arranged in a row to establish normal contact between adjacent dwellings, representing the interconnected nature of these configurations. The analysis reveals significant variations in response between isolated and aggregated setups. Furthermore, the seismic capacity of systems within the aggregate differs based on their position, with distinct resistance and failure mechanisms observed among dwellings. This research provides valuable insights into the seismic performance of modern aggregate masonry systems, underscoring the importance of inter-dwelling connections in densely populated urban areas exposed to high seismic activity. The findings contribute to the development of effective strategies for designing, assessing, and retrofitting such systems, thereby enhancing resilience and safety in seismic-prone regions.*

1. Introduction

The predominant focus of research concerning aggregated structures has traditionally revolved around unreinforced masonry systems within seismic regions, particularly in historic European centres such as those found in Italy or Portugal. These investigations have explored diverse aggregate configurations, encompassing rows (Angiolilli et al., 2021; Battaglia et al., 2021) and irregular layouts (Grillanda et al., 2020). Additionally, these studies have considered dwellings characterized by either a single shared wall or perfectly joined contiguous walls, a standard layout in these historic centres (Angiolilli et al., 2021).

Research on aggregates in historic centres has determined that earthquake effects on each unit vary based on their position within the ensemble, primarily due to torsion effects resulting from both local and global geometries. For example, a seismic vulnerability study of an extended aggregate comprising nine historic different unreinforced masonry buildings (Greco et al., 2020) revealed that the ensemble exhibited higher

longitudinal resistance than individual buildings, likely due to confinement effects. However, resistance in the transverse direction decreased for some structures. Additionally, the smaller inner units experienced significant reductions in resistance when subjected to relative displacements caused by adjacent larger buildings.

Similarly, previous research noted the concentration of highest shear stresses on the walls of end units in row configurations (Battaglia et al., 2020; Valente et al., 2019) and on corner units in block-type aggregates (Formisano et al., 2010). This study also introduced an adjusted vulnerability index to account for structural interactions between neighbouring buildings, subsequently applied in related studies (Chieffo and Formisano, 2019) showing that the probability of damage was lower in the aggregate compared to isolated units and that corner units were more susceptible to seismic activity than intermediate ones.

Research on aggregate systems has expanded to encompass various construction methods and contemporary building complexes. For instance, Marques et al. (2012) investigated a row-shaped aggregate of bed-joint reinforced concrete masonry constructions by means of macro-elements, while Torres-Olivares et al. (2023) also studied a row-shaped aggregate but of modern-type partially grouted reinforced concrete masonry (PG-RCM), assessing the contact-like interaction widely observed using an equivalent frame model.

Angiolilli et al. (2023) introduced an innovative procedure that considers the effects of pounding in the global response of structures within a row aggregate. This procedure delves into the interaction and contact between neighbouring structures. When assessing the seismic safety of aggregates, it is crucial to consider boundary conditions, especially those associated with the interaction of structural units. This interaction involves both the internal and external behaviour of each unit, wherein the quality of connections between adjacent buildings plays a pivotal role. However, numerically simulating these connections remains an underexplored task within this field.

As mentioned before, prior research has mainly focused on the behaviour of aggregates in European urban areas with medium-to-high seismic hazards but hasn't addressed regions with high seismic risk, such as Central America. In these countries, the predominant construction systems differ from traditional systems studied elsewhere. For example, San José, the capital of Costa Rica, is an important urban centre located in an active seismic zone affected by subduction (interplate and intraslab) and active shallow crustal earthquakes. The construction system there relies on partially grouted concrete block masonry walls, but local construction practices substantially vary from other regions.

Despite mounting evidence suggesting that aggregate structures respond differently to seismic loading compared to isolated ones, current seismic codes in Costa Rica predominantly concentrate on the behaviour of isolated buildings. The current design assumes that PG-RCM buildings function in isolation, despite potential interactions between adjacent structures impacting seismic capacity and failure mechanisms (Torres-Olivares et al., 2023). Consequently, there exists a lack of regulatory clarity and research-based guidance on designing and evaluating the seismic performance of aggregated buildings in Costa Rica. Investigating the seismic behaviour of commonly used PG-RCM houses in aggregate configurations is vital to address this knowledge gap.

The primary aim of this research is to investigate the collective behaviour of contemporary partially grouted reinforced concrete systems. Specifically, the study aims to analyse how these modern structures behave when aggregated in the widely observed wow-shape manner, delineate observed failure mechanisms, and compare these findings with the seismic response of isolated units.

This study employs a finite element macro-modelling approach to represent the masonry material and study the nonlinear dynamic behaviour of current PG-RCM aggregate residences. It considers the typical contact conditions representative of modern construction practices. Furthermore, the research delves into the behaviour of individual units within the aggregate, providing deeper insights into the interaction effects between neighbouring structures and the mechanisms leading to failure.

2. Model description

The material modelling for this study was performed using the OpenSees software (McKenna, Scott & Fenves, 2010), in conjunction with the STKO (Petracca et al., 2017) pre and post-processing software. To represent the masonry material, the plastic damage model ASDConcrete3D (Petracca, 2023) was employed. The modelling of the system, which involved partially grouted reinforced concrete block masonry, was carried out using a macro-

modelling with smeared rebars strategy. This approach used a homogenised material representation, which was chosen for its ability to accurately simulate material behaviour while effectively managing computational costs.

Vertical and horizontal reinforcements within the walls were treated as smeared rebars, with the material properties of the steel described using the Steel02 model, subsequently implemented as PlateRebar. The masonry itself was represented as PlateFiber, resulting in the wall being modelled as a LayeredShell with distinct layers with equivalent thicknesses for masonry and reinforcements.

Because the area of steel is considered as a plate element that is perfectly integrated as an additional layer in the wall shell, this leads to an overestimation of the strength, particularly for horizontal reinforcement, as the bars are placed in the mortar bed between blocks. This issue has been addressed in the study by Hidalgo-Leiva et al. (2021), which reduced the contribution of steel in shear by 50%. Similarly, for this study, it has been decided to consider an effective area of 50% of the steel shear reinforcement area. For vertical reinforcement, no reduction has been applied, as the bars are embedded within the wall and covered by grout.

This choice of materials and modelling approaches aligns with the aim of achieving scientific rigour and computational efficiency in the study. The selection of a homogenised material representation and shell elements not only serves to capture the material behaviour realistically, but also to allow for the observation of failure mechanisms, including out-of-plane resistance. This is particularly crucial for accurately simulating the interactions between adjacent structures within the aggregate. Moreover, this approach maintains a lower computational burden compared to three-dimensional elements, ensuring both accuracy and computational efficiency in investigating the behaviour of buildings within the aggregate. These material properties were derived from experimental data sources, as described by Hidalgo-Leiva et al. (2021), further enhancing the credibility of the model.

The interactions between the housing units are established by assuming full contact between the walls of adjacent structures. An interaction is performed in which the larger dimension wall is treated as the master nodes, while the smaller dimension wall is regarded as the slave nodes. To create a frictionless contact, an Elastic Perfectly Plastic Gap Uniaxial material with the ElasticPPGap material, is employed. This material is considered elastic with an initial gap of 0 and a high elasticity modulus. The material is used to construct zeroLength element objects, which will exclusively act perpendicular to the walls. The described contact is shown in Figure 1 in red.

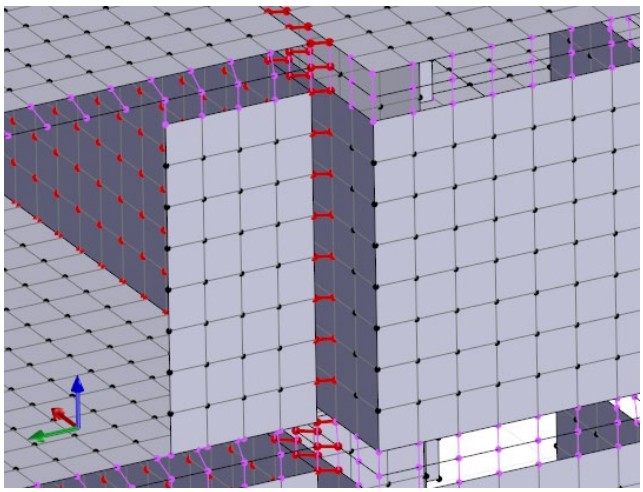

Figure 1. Example of contact created between nodes of adjacent structures.

2.1. Validation of masonry model

To validate the chosen modelling approach, an initial step involved the development of a numerical model, based on the experimental investigation conducted by Hidalgo-Leiva et al. (2016). The wall under investigation is constructed using concrete masonry blocks measuring 120 × 390 × 190 mm in size. The experimental setup and configuration are depicted in Figure 2(a), showing the position of the reinforcement bars in colour red, providing a visual representation of the studied specimen. Additionally, Figure 2(b) illustrates the cracking pattern observed in the experimental tests for the wall.

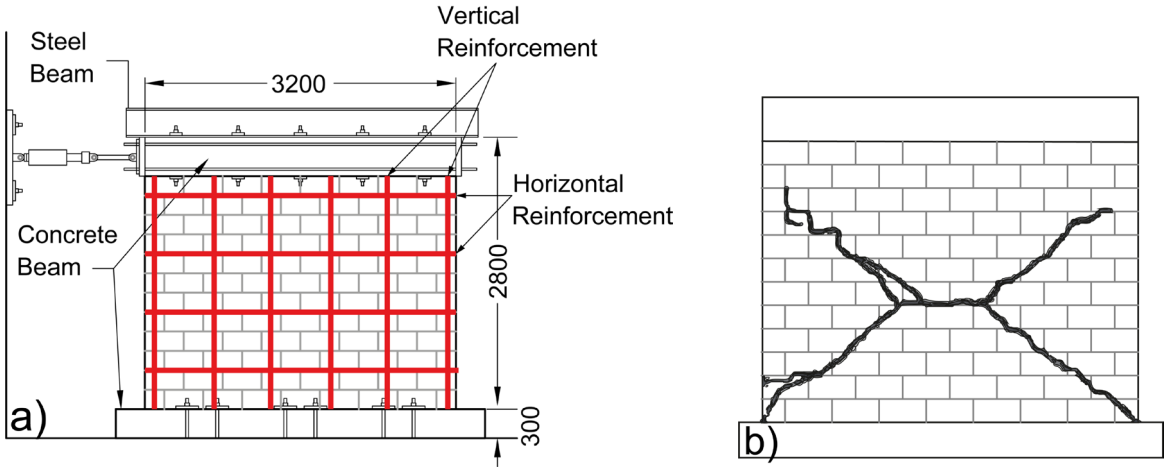

Figure 2. Experimental setup and crack pattern observed, adapted from Hidalgo-Leiva et al. (2016).

As described in Hidalgo-Leiva et al. (2016), the material properties obtained experimentally are: Compressive resistance of masonry $f'_m = 12.6\ [MPa]$, Vertical reinforcement (grade 60) yield strength $f_{y60} = 506\ [MPa]$ and horizontal reinforcement (grade 40) yield strength $f_{y40} = 367\ [MPa]$. The assumed homogenised masonry material response to cyclic uniaxial loading is depicted in Figure 3.

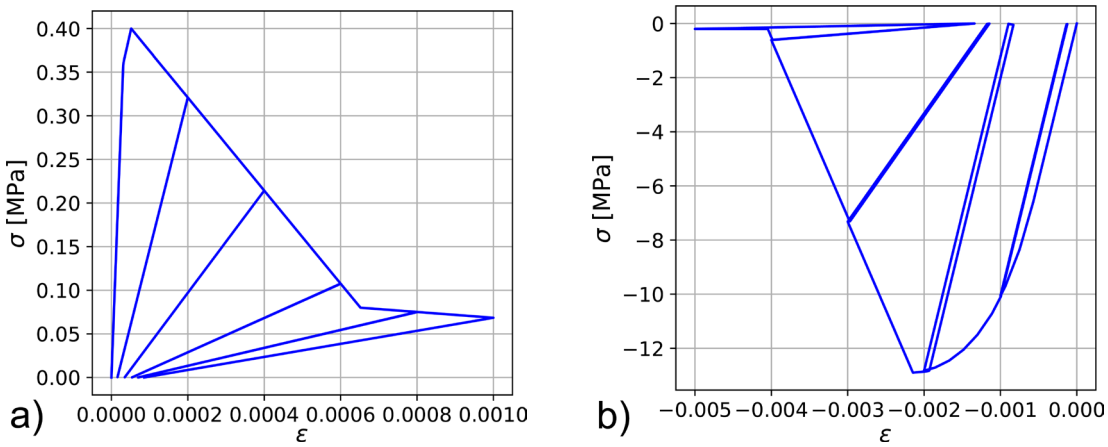

Figure 3. Material used to macro-model partially grouted concrete block masonry. stress-strain hysteretic curves.

The finite element model undergoes a pseudo-static cyclic analysis, considering the imposed displacement corresponding to the loading protocol used in the experimental test. Displacements are applied to the top of the wall, while the base is considered fixed. Subsequently, the results are presented in Figure 4(a). Figure 4(b) displays the crack pattern obtained numerically for the finite element model (values in millimetres), with colours representing the size of cracks in the material.

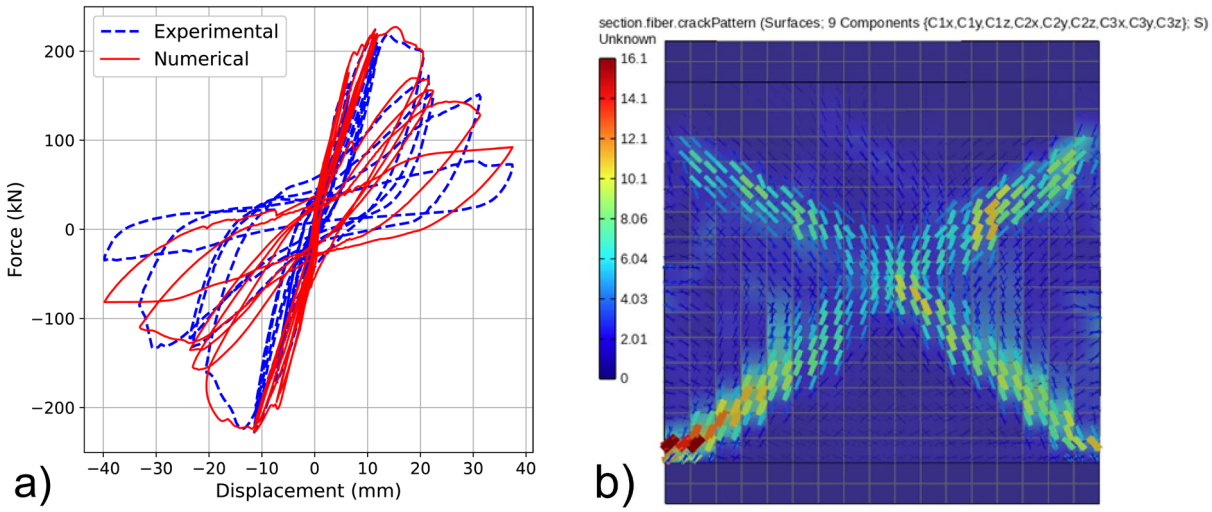

Figure 4. Numerical results obtained for the wall FE model.

The type of failure in the plane of the wall corresponds to the shear failure pattern, with cracks similar to what has been observed experimentally and what is expected for a wall of these characteristics.

3. Seismic behaviour of aggregated reinforced masonry buildings

3.1. Isolated structure dynamic analysis

The structure investigated in this study corresponds to the one examined by Hidalgo-Leiva et al. (2021), shown in Figure 5(a). It is constructed using partially reinforced concrete block masonry walls, with walls measuring 12 centimetres in thickness. The slabs are constructed in a manner that allows them to be considered rigid diaphragms.

A finite element model of the structure is created, considering the walls with the previously validated material model and the crown beams as Beam elements connected to walls and floors considering equaldof condition between nodes.

In the finite element model, a 1% Rayleigh numerical damping is applied because, in the early stages of the earthquake, the walls behave elastically, and some dissipation is necessary. The structure undergoes a non-linear dynamic analysis. For this purpose, mass is assigned to the shell elements of the slabs and walls in all three global directions. A regular mesh size of 300 millimetres square elements has been considered. This size allows for obtaining satisfactory results while maintaining low computational costs. Figure 5(b) depicts the finite element model.

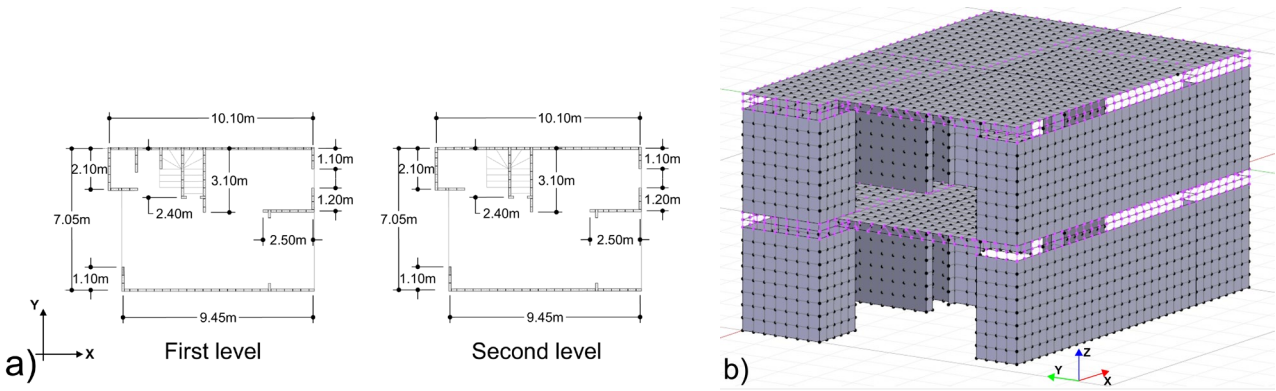

Figure 5. Plan view and finite element model mesh.

The seismic record from Kobe (1995), extracted from the Pacific Earthquake Engineering Research Center (PEER) Ground Motion Database, is considered, encompassing its two horizontal directions. It has been decided to use twice the amplitude of the seismic motion, i.e., 1.20(g) and 1.64(g) of peak ground accelerations, thus ensuring element failure, with the major component positioned in the weak direction of the structure (Y-axis). The seismic record is applied at the base of the structure as an acceleration input.

To calculate the relative roof displacement, the average displacement of all roof nodes has been considered, with the average displacement of all base nodes subtracted. It's important to note that this approach does not account for the torsional effects present in the structure and only provides a relative idea of its displacement. Hysteresis curves for X and Y direction are shown in Figure 6(a) and 6(b) respectively.

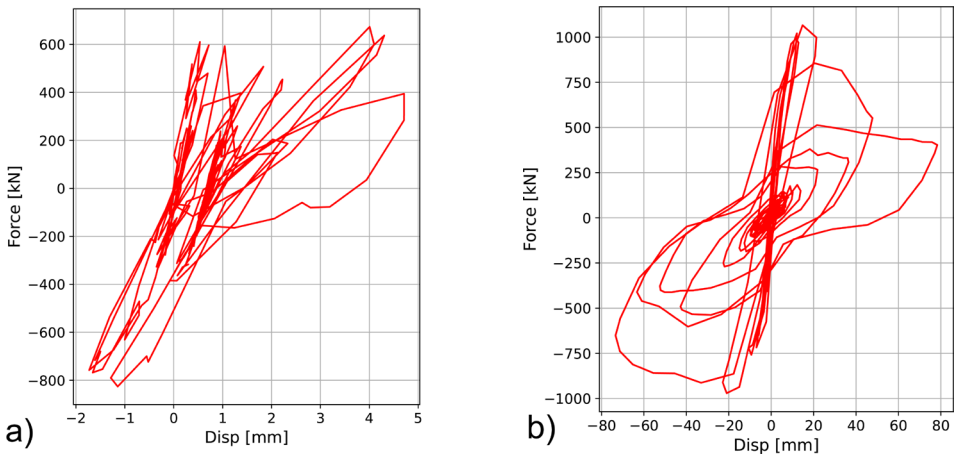

Figure 6. Hysteresis curves of the isolated structure.

From results of the dynamic analyses, it is possible to observe that the largest displacements are observed in the weak axis of the structure (Y-axis). This is observed, on one hand, because the strongest component of the earthquake is oriented in this direction, and on the other hand, because the deformations of the structure tend to concentrate in the weakest direction.

Due to these displacements, the damage has concentrated in the walls of the Y-axis, as shown in Figure 7. Here, in red, the crush pattern is depicted, while black highlights the crack pattern. This is done to identify the walls that experience shear damage and those exhibiting bending damage. Walls experiencing bending-type failures are identified mainly by crushing at the corners of the walls. Shear-type failures are mainly observed as diagonal cracks in the centre of the walls or as horizontal cracks corresponding to shear sliding failure at the base. Note that both scales are in millimetres and set to a minimum of 0.5 and maximum of 10.

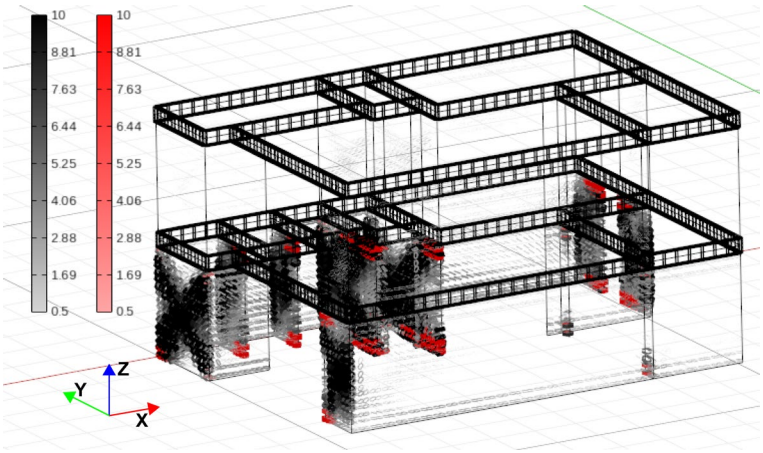

Figure 7. Crack (black) and crush (red) pattern at the end of loading in millimetres. Isolated structure.

It is important to note that the walls along the X-axis display small cracks with a horizontal distribution and do not show any signs of crushing failure. On the other hand, the walls along the Y-axis clearly exhibit signs of crushing at the corners, along with noticeable diagonal cracks. In the case of unreinforced masonry, it is easier to identify the types of failures, whether due to shear or bending. However, in reinforced masonry, due to the presence of steel bars, the wall continues to bear loads after the initial masonry failure. This leads to a state in which the element is in a combination of shear and bending failure, and it is not always evident which of these failures is more predominant than the other.

3.2. Aggregated structures dynamic analysis

For the current study, five identical structures are considered, arranged in an aggregated manner with their lateral walls positioned adjacent to each other, each dwelling has a number assigned, as shown in Figure 8.

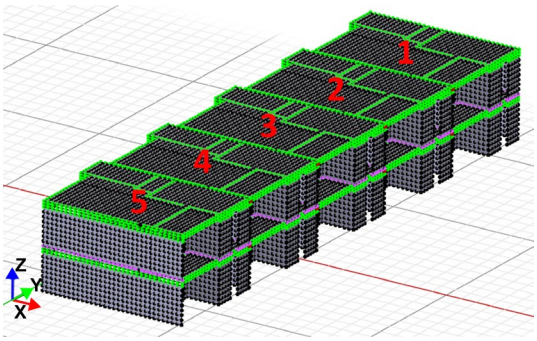

Figure 8. Enumeration of the structures along the aggregate.

In Table 1, the values obtained for relative roof displacements and base shear are shown for the isolated structure and each of the structures that make up the aggregate. Similar to the isolated structure, the aggregated structures experience higher shear forces and larger displacements in the Y-axis direction compared to the X-axis.

Table 1. Base shear and roof displacement at peak resistance and maximum roof relative displacement.

Structure	**Peak base shear [kN]**		**Roof disp. at peak [mm]**		**Max. roof disp. [mm]**	
	X-axis	**Y-axis**	**X-axis**	**Y-axis**	**X-axis**	**Y-axis**
Isolated structure	826.18	1065.99	1.15	14.79	4.71	78.28
Dwelling 1	957.64	1083.16	2.85	11.13	4.43	60.29
Dwelling 2	998.81	1118.95	3.28	11.02	4.40	46.93
Dwelling 3	1002.43	1126.23	3.34	10.92	4.35	46.95
Dwelling 4	1016.80	1104.36	3.03	10.87	4.31	47.01
Dwelling 5	1003.96	1116.13	3.63	10.82	4.43	47.36

The results indicate that the maximum displacements, representing the peak roof displacements recorded during the analysis, are greater in both directions (X-axis and Y-axis) for the isolated structure in comparison to the aggregated dwellings. This suggests that the interaction between the structures in the aggregate may contribute to a reduction in the maximum displacements.

In the aggregate, maximum displacements are larger at the ends for both axes, aligning with literature that suggests structures located at the ends of a linear aggregate are more vulnerable during an earthquake. Specifically, Dwelling 1 exhibits substantially larger displacements than the other dwellings on the Y-axis.

Regarding base shear, it is evident that base shear values in both the X and Y directions increase from the isolated structure to all dwellings in the aggregate. This suggests that structures in the aggregate experience higher shear forces due to their interaction during an earthquake.

The displacement at peak base shear in the X-axis direction exhibits a clear increase from the isolated structure to the dwellings in the aggregate. However, in the Y-axis direction, the isolated structure has a higher displacement at peak base shear compared to any of the dwellings in the aggregate.

When examining secant stiffness at the peak value (displacement at peak over peak base shear), there is a trend toward higher values at one end (Dwelling 5) of the aggregate compared to the other end (Dwelling 1) in the Y-axis direction. This could indicate a non-uniform distribution of stiffness along the aggregate. Additionally, a stiffening effect is observed in the Y-axis direction, and a reduction of stiffness is observed in the X-axis direction when the structures are aggregated. This might be related to the orientation of structures and their interaction during an earthquake.

Calculating percentage changes from the isolated structure to each dwelling in the aggregate, there is an increase of approximately 16% to 23% in base shear (X-axis), 1.6% to 5.7% in base shear (Y-axis), 149% to 217% in displacement at peak base shear (X-axis), and a decrease of approximately 25% to 27% in displacement at peak base shear (Y-axis), 6% to 8% in maximum roof displacement (X-axis), and 23% to 40% in maximum roof displacement (Y-axis).

Figure 9 shows cracks in black and crush in red on the masonry at the end of the dynamic analysis. Note that both scales are in millimetres and have been set to a minimum value of 0.5 and maximum of 10.

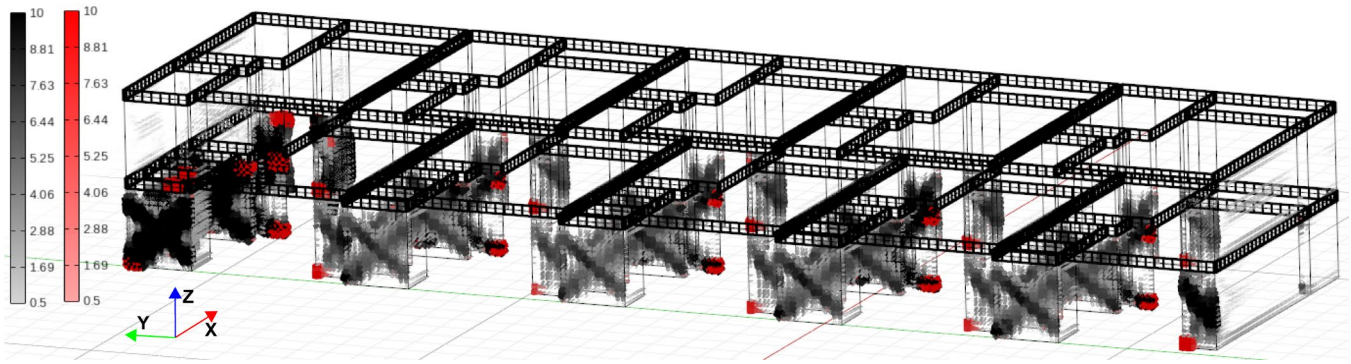

Figure 9. Crack (black) and crush (red) pattern at the end of loading in millimetres. Aggregated structures.

Finally, Figures 10 and 11 depict the crack and crush patterns, respectively, for the aggregated and the isolated structure, using the same scale (in millimetres) in the final step of the analysis.

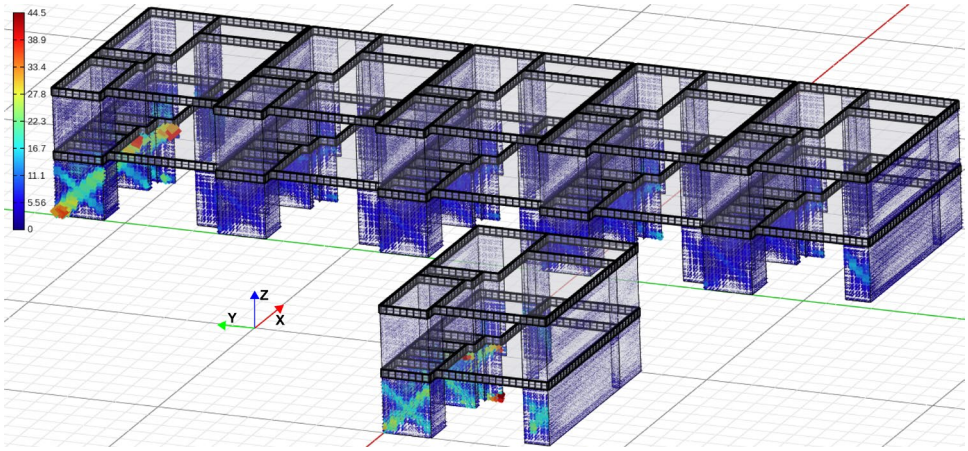

Figure 100. Comparison of crack pattern for isolated and aggregated structures. Scale in millimetres.

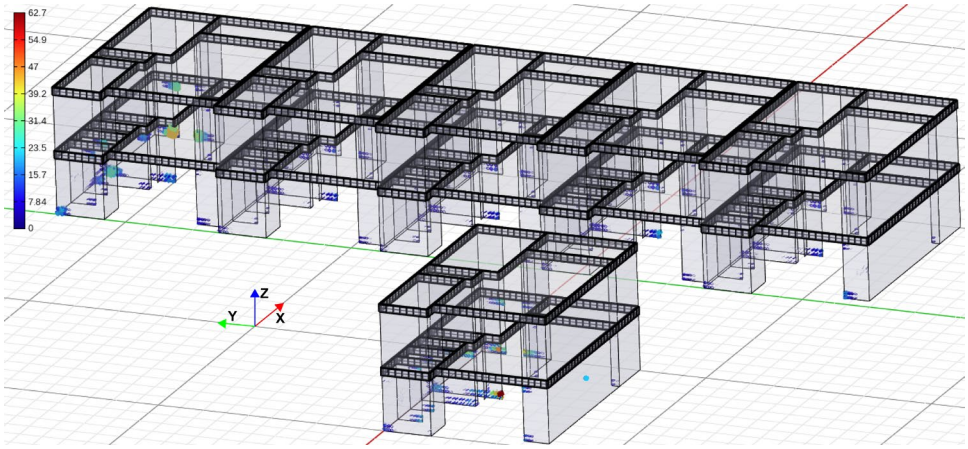

Figure 11. Comparison of crush pattern for isolated and aggregated structures. Scale in millimetres.

As an initial observation, the aggregated structures exhibit a higher presence of cracking in the walls along the X-axis than the isolated structure. Additionally, it can be observed that the maximum value in both graphs is found on one of the internal walls of the isolated structure. However, House number 1 exhibits higher values of cracking and crushing in other walls, also with a notably greater density of cracks. It is also worth noting that, despite reaching higher peak shear values, as shown in Table 1, dwellings from 2 to 5 display considerably fewer cracks and even less crushing compared to the isolated structure. This makes sense as the maximum displacements of the aggregated buildings are lower than those of the isolated structure. Given this and considering that the models of the dwellings are identical, the aggregated structures exhibit some energy dissipation mechanism does not present in the isolated structure. This raises the possibility that the aggregated dwelling may be dissipating energy through the accumulation of damage in dwelling 1.

4. Conclusions

The modelling strategy used is capable of satisfactorily representing the studied construction typology. A change in the response of the structures is observed when they are in their aggregated condition. Furthermore, there is a difference in the behaviour of each of the structures. An increase in the stiffness of the structures in the direction of the aggregate of approximately 40% and a reduction in stiffness in the direction perpendicular to the aggregate of approximately 60% are observed. In general, reinforced masonry walls, exhibit a combination of failure modes, which can complicate the evaluation of their wall strength using traditional methods that consider only one failure mode at a time and remark the advantage of the employed model. The aggregate-like behaviour of the structures in line tends to concentrate damage at one end, which appears to result in an energy dissipation mechanism for the structures in contact.

As future research, the evaluation and comparison of energy dissipation in different structures and the assessment of more heterogeneous aggregates are proposed.

5. Acknowledgments

Sebastian Torres-Olivares acknowledges the financial support from Agencia Nacional de Investigación (ANID), Subdirección de capital humano, Magíster nacional 2022, Chile, Folio 22221341. The authors are grateful to UE project 9063-01 Adelante 2 " Sustainable and resilient construction in Central America and the Caribbean in the face of seismic risk: regional cooperation based on the experience of Costa Rica" for supporting the research.

6. References

Angiolilli M., Brunelli A., Cattari S. (2023). Fragility curves of masonry buildings in aggregate accounting for local mechanisms and site effects, *Bulletin of Earthquake Engineering*, 21(5):2877–2919.

Angiolilli M., Lagomarsino S., Cattari S., Degli Abbati S. (2021). Seismic fragility assessment of existing masonry buildings in aggregate, *Engineering Structures*, 247:113218.

Battaglia, L., Buratti, N., Savoia, M., 2020. Seismic fragility assessment of masonry aggregates with identical structural units in row, In: Kubica, J., Kwiecien, A. & Bednarz, L., eds. Brick and Block Masonry - From Historical to Sustainable Masonry. 1st ed. CRC Press, pp.908-915.

Battaglia L., Ferreira T. M., Lourenço, P. B. (2021). Seismic fragility assessment of masonry building aggregates: A case study in the old city Centre of Seixal, Portugal, *Earthquake Engineering & Structural Dynamics*, 50(5):1358–1377.

Chieffo N., Formisano A. (2019). Comparative Seismic Assessment Methods for Masonry Building Aggregates: A Case Study, *Frontiers in Built Environment*, 5:123.

Formisano, A., Landolfo, R., Mazzolani, F.M., Florio, G., 2010. A quick methodology for seismic vulnerability assessment of historical masonry aggregates, *Proceedings of the COST action C26 final conference "Urban Habitat Constructions Under Catastrophic Events"*, Naples, Italy.

Greco A., Lombardo G., Pantò B., Famà A. (2020). Seismic Vulnerability of Historical Masonry Aggregate Buildings in Oriental Sicily, *International Journal of Architectural Heritage*, 14(4):517–540.

Grillanda N., Valente M., Milani G., Chiozzi A., Tralli A. (2020). Advanced numerical strategies for seismic assessment of historical masonry aggregates, *Engineering Structures*, 212:110441.

Hidalgo-Leiva D., Barbat A., Pujades L., Acuña-García D. (2016). Experimental analysis of in-plane shear strength of reinforced concrete masonry walls and its seismic behavior, In: Modena, C., da Porto, F. & Valluzzi, M., eds. Brick and Block Masonry. 1st ed. CRC Press, pp.2295-2302.

Hidalgo-Leiva D. A., Pujades L. G., Barbat A. H., Vargas Y. F., Díaz S. A. (2021). Nonlinear static and dynamic analyses of Costa Rican reinforced concrete masonry structures, *Engineering Structures*, 234:111998.

Marques R., Vasconcelos G., Lourenco P. (2012). Pushover analysis of a modern aggregate of masonry buildings through macro-element modelling, *15th International Brick and Block Masonry Conference*. Florianopolis, Brazil.

McKenna, F., Scott, M.H., Fenves, G.L., 2010. Nonlinear finite element analysis software architecture using object composition. *Journal of Computing in Civil Engineering*, 24(1), pp.95-107.

Petracca, M., Candeloro, F., and Camata, G. (2017). STKO user manual. ASDEA Software Technology, Pescara, Italy.

Petracca, Massimo. (2023). ASDConcrete3D Material Model. In OpenSees. Available at: https://opensees.github.io/OpenSeesDocumentation/user/manual/material/ndMaterials/ASDConcrete3D.html (Accessed: 28 October 2023).

Torres-Olivares S., González-Rodrigo B., Saavedra-Flores E. I., Mosquera-Feijoo J. C. (2023). Seismic behaviour of reinforced-masonry aggregate under different types of interaction between adjacent dwellings, *Bulletin of Earthquake Engineering*.

Valente M., Milani G., Grande E., Formisano A. (2019). Historical masonry building aggregates: Advanced numerical insight for an effective seismic assessment on two row housing compounds, *Engineering Structures*, 190:360–379.